2008 IEEE International Conference on
Robotics and Automation
Pasadena, CA, USA, May 19-23, 2008

Use of a Novel Multipart Controller for the Parametric Study of a Trotting Quadruped Robot

Nicholas Cherouvim and Evangelos Papadopoulos, *Senior Member, IEEE*

***Abstract*— In this paper a novel multipart control is developed for a trotting quadruped robot. The control is designed to drive the quadruped to a steady-state motion with desired forward speed and apex height, using only one actuator per leg. The body pitching motion is controlled to be small. The controller is applied to the robot and the complete system is used to develop a parametric study for the robot. The study examines the behavior of the actuator effort and the leg touchdown angles, over a parametric region of both the robot physical parameters and the gait parameters. Interesting results appear, not previously reported, that may contribute to enhanced robot design and better gait selection for a given robot. Typical findings are that a robot should be lighter-weight when running on more slippery terrain, as well as that certain higher forward speeds require less actuator effort than other slower speeds.**

I. Introduction

CONSIDERABLE research has recently focused on the control and design of quadruped legged robots that are capable of dynamic locomotion. Widely different approaches have been followed to successfully control the robots. To name a few approaches, a form of PD control has been used [1], and also delayed feedback control has been applied [2]. Further, a number of quadruped designs have been realized, with very different physical parameters, such as body mass, leg length, etc. Some of these are the Tekken [3], BigDog [4], and KOLT [5] robots.

An interesting issue in legged robots, that still remains relatively untouched, is the effect of gait characteristics, such as forward speed and apex height, and robot physical parameters, on key quantities of the robot motion. Such key quantities are the actuator effort and the leg touchdown angles. Specifically, it still remains to be seen how such quantities vary for some parametric range of robot physical parameters and gait characteristics, and whether the nature of this variation makes some parametric regions more desirable than others. Also, the underlying mechanisms of such variations have yet to be fully explored.

The actuator effort required to sustain the motion of a quadruped robot, see Fig. 1a, determines the minimum size of the robot actuators. Also, the magnitude of the leg touchdown angles greatly affects the likelihood of slipping. Therefore, the unveiling of how the actuator effort and the leg touchdown angles change across the parametric region of the robot physical parameters and the gait characteristics could facilitate improved robot design and the matching of a more suitable gait to a given robot. Some work in this direction was done in [6], although this considered a one-legged robot and did not study a parametric region of robot physical parameters, only of gait characteristics. For this work, we adopt a planar quadruped model with a unit dimensionless inertia, similar to the models used in [7,8] which study dynamic properties of quadruped robots.

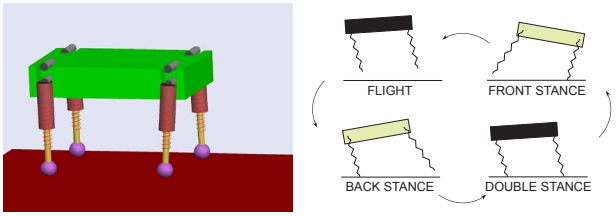

(a) (b)

Fig. 1 (a) Quadruped robot and (b) trotting gait phases *in the plane*. Only the phases in which the robot is colored black are present in ideal trotting.

In this work we first develop a novel multipart controller that drives a trotting quadruped to some desired forward speed and apex height. The control retains the pitching motion to a minimum, and uses only *one* actuator per leg. It has a parametric form that allows it to be applied to a range of robots with different physical parameters. This control is used to perform a parametric study on the quadruped robot. The aim of the parametric study is to unveil how the actuator effort and the leg touchdown angles change for ranges of physical robot parameters and gait characteristics. The study examines the case of robot design for a particular gait, as well as the evaluation of gait suitability for a particular robot. The study unveils interesting trends which are discussed and compared to results in the literature. One example has to do with how the mass of a robot should be modified for running on lower-friction terrain. Section II follows to present the robot model used in this work.

II. Quadruped Robot Model

A. Quadruped Robot

The quadruped robot studied has the form shown in Fig. 1a. The robot is purposely simple and incorporates basic elements that are found in the majority of legged robots.

This work is co-funded by public funds (European Social Fund 75% and General Secretariat for Research and Technology 25%) and private funds (Zenon S.A), within measure 8.3 of Op.Pr.Comp., 3rd CSP - PENED 2003.

N. Cherouvim is with the Department of Mechanical Engineering, National Technical University of Athens, Athens, 15780, Greece. (e-mail: ndcher@mail.ntua.gr, phone: +(30) 210-772-2643).

E. Papadopoulos is with the Department of Mechanical Engineering, National Technical University of Athens, Athens, 15780, Greece (e-mail: egpapado@central.ntua.gr, phone: +(30) 210-772-1440, fax: +(30) 210-772-1455).

Each leg of the robot has a prismatic joint with a linear spring to provide compliance, and each hip is actuated. By using a simpler model, the conclusions of the parametric study are more general than they would be from studying a more specific robot case. Note that virtually all quadruped robots that are capable of dynamic locomotion have a hip joint, a hip actuator and some sort of passive compliance in the leg, as does the robot studied here.

A quantity of known importance in the literature is the dimensionless inertia of the robot body, which is defined as:

$$J = I/(md^2) \tag{1}$$

where I is the body inertia that is relevant to the pitching motion, m is the body mass, and d is half the hip spacing.

In this work, the dimensionless inertia of the robot is chosen to be 1. This choice is inspired by the work in [9], in which the stability of a quadruped model was studied for the pronking gait, used as an abstraction of the trotting gait in the plane. In [9] it was found that a dimensionless inertia of 1 provided a very wide range of stable pronking (or planar trotting) motions when compared with cases for which the dimensionless inertia was less than one. Further, in this paper we make use of the pitch motion control set out in [10], in which a unit dimensionless inertia was shown to have advantages in pitch control. It is simple for a robot to attain a specific value of dimensionless inertia by proper hip placement or redistributing body mass.

B. Planar Model Dynamics

The robot is studied in the plane of the forward motion for the case of the trotting gait. In the ideal case, the two diagonal pairs of the four legs are always in phase. During a stance phase, a diagonal pair of legs is on the ground, while the remaining pair is not in contact. The pair of legs in contact with the ground alternates after each stance phase. Projecting this on to the plane of the forward motion, results in the configuration shown in Fig. 2. The trotting gait is shown in the plane in Fig. 1b with four phases, although in ideal trotting only the double stance and flight phases exist. The two legs shown may be either of the diagonal pairs of the robot that are in contact with the ground. The legs that are not in contact are not shown.

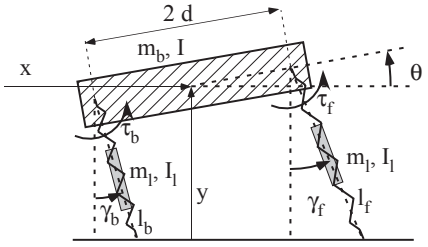

Fig. 2 Planar quadruped robot model.

In Fig. 2, the body has its center of mass (CoM) at its geometrical center. The legs each have total mass m_l, inertia I_l, and are actuated by torques τ_f, τ_b at the two hips. Each leg includes viscous friction in the prismatic joint, of viscous coefficient b. Table 1 displays variables and indices used.

During the stance phase, the influence of the leg mass is negligible, and the dynamics may be derived with a Lagrangian approach, using body Cartesian coordinates, x, y, and pitch, θ, as generalized variables:

$$\frac{d}{dt}\begin{bmatrix}\mathbf{q}\\ \dot{\mathbf{q}}\end{bmatrix} = \begin{bmatrix}\dot{\mathbf{q}}\\ -\mathbf{M}^{-1}(\mathbf{F_{k,b}}+\mathbf{F_{k,f}}+\mathbf{F_{b,b}}+\mathbf{F_{b,f}}+\mathbf{G})\end{bmatrix} \tag{2}$$

where $\mathbf{q} = [x \quad y \quad \theta]^T$, $\mathbf{M}$ is the mass matrix, $\mathbf{G}$ are the gravity dependent terms, $\mathbf{F_{k,i}}$ are due to elastic leg forces and $\mathbf{F_{b,i}}$ are leg related forces due to the viscous friction in the prismatic leg joint ($i = b, f$ for the back and front leg).

In flight, the system CoM performs a ballistic motion. Also, the angular momentum of the system of the body and legs, with respect to the system CoM, is conserved.

Further, with reference to Fig. 2, it is useful to associate the Cartesian coordinates with the leg lengths and leg angles during the stance phase when two legs are on the ground:

$$\gamma_b = \tan^{-1}(y - d\sin\theta, x_{bt} + d\cos\theta - x) \tag{3}$$

$$\gamma_f = \tan^{-1}(y + d\sin\theta, x_{ft} - d\cos\theta - x) \tag{4}$$

$$l_b = \sqrt{(-x + x_{bt} + d\cos\theta)^2 + (y - d\sin\theta)^2} \tag{5}$$

$$l_f = \sqrt{(-x + x_{ft} - d\cos\theta)^2 + (y + d\sin\theta)^2} \tag{6}$$

where x_{bt} is the position of the back foot, x_{ft} is the position of the front foot during the double stance phase.

TABLE 1
VARIABLES AND INDICES USED IN THE WORK

x	CoM horizontal position	L	leg rest length
y	CoM vertical position	b	viscous friction coefficient
θ	body pitch angle	g	acceleration of gravity
l	leg length	m_l	leg mass
γ	leg absolute angle	I_l	leg inertia
γ_{sum}	sum of leg absolute angles	$\gamma_{b,td}$	back leg touchdown angle
γ_{dif}	difference of leg absolute angles	$\gamma_{f,td}$	front leg touchdown angle
k	leg spring stiffness	τ	hip torque
m_b	body mass	T_{st}	stance duration
m	total robot mass	f	*as index*: front leg
I	body inertia	b	*as index*: back leg
d	hip joint to CoM distance	td	*as index*: value at touchdown

III. CONTROL DESIGN

In this section, we present a novel control approach for the quadruped robot, which will facilitate the parametric study in Section IV. The control is designed to control both the forward speed and the apex height attained during the flight phase. The pitching motion is kept to a minimum, so as to be compatible with the trotting gait. Also, only one actuator is used per robot leg. Finally, the control has a parametric form and can be simply applied for a range of robot physical parameters and gait characteristics. No tuning is required as all control parameters are analytically computed. To the best of our knowledge, a controller with these capabilities does not exist in the literature.

To relieve the paper of cumbersome math and to focus on the parametric study, we endeavor to make use of our previous analysis in [10]. Note that [10] does not provide a

complete control method, but rather an analysis of the dynamics and a control method for the pitching motion. Here, we use these results to develop a complete controller. Also, the gait studied in [10] was pronking, however the model used was the same as the one used here.

As a design decision, the torques applied at the back and front hips during the stance phase will be equal and constant throughout the stance phase, although the constant value may change from cycle to cycle. Three control inputs are available, namely the back and front leg touchdown angles and the equal hip actuator torques during stance, τ . During flight, the hip actuators position the legs for touchdown.

Our approach for the derivation of the control strategy follows the philosophy of the multipart approach introduced by Raibert [7]. The problem of controlling the complete robot motion is split into separate subproblems. Each subproblem deals with controlling a particular elementary motion of the robot. In our robot, the three elementary motions are the vertical, the forward and the pitching motions. Our approach differs from [7], as we use only one actuator per leg, and do not need the concept of "virtual legs". Also, as our robot is highly underactuated, we must consider the effect of the control inputs on multiple degrees of freedom (DoF), and the effect of one DoF on another.

To formulate the mathematical aspect of the control, we make use of our previous analysis in [10]. In this previous work, after some algebra, we arrive at an expression that describes each of the elementary motions. We use here directly these expressions to compute the control inputs.

A. Vertical motion

Starting from the dynamics in (2), and using (3) to (6), it is found that the vertical motion of the robot during the double stance phase is well described by the following, [10]:

$$m_b\ddot{y}+2b\dot{y}+2ky=-m_bg+2kL\cos\left(\frac{\gamma_{sum,td}}{2}-\frac{\dot{x}t}{L}\right)\cos\left(\frac{\gamma_{dif,td}}{2}\right) \quad (7)$$

where $\gamma_{sum,td}$ is the sum of the leg touchdown angles, $\gamma_{dif,td}$ is the difference of the leg touchdown angles.

The physical meaning of (7) is revealed by noting that the vertical motion is governed by a driven oscillator. In trotting, $\gamma_{dif,td}$ is small enough to have little influence in the cosine. Therefore, (7) can be rewritten as:

$$m_b\ddot{y}+2b\dot{y}+2ky=-m_bg+2kL\cos\left((\gamma_{sum,td}/2)-(\dot{x}t/L)\right) \quad (8)$$

Given the initial conditions for y, (8) may be solved. The required calculation of the duration of the stance phase is accomplished as in [10]. Then, (8) is used to compute $\gamma_{sum,td}$, such that the robot acquires some desired vertical liftoff velocity or, equivalently, some attained apex height. The solution is provided by function f_1:

$$\gamma_{sum,td}=f_1(\underbrace{m,k,L,d,I,b,g}_{\text{robot parameters}},\ \underbrace{\dot{x}_{des},h}_{\text{gait parameters}}) \quad (9)$$

B. Forward motion

The forward motion equation, as found in [10], is:

$$m_b\ddot{x}=-k\left(L-y\right)\sin\left(\gamma_{sum,td}-2\dot{x}t/L\right)-(\tau_b+\tau_f)/L \quad (10)$$

In (10), the forward dynamics is coupled with the vertical motion of the robot. This is easily interpreted as being due to the influence of the prismatic leg springs on the forward motion of the robot. From (10) it is sought to compute the necessary hip torque τ during stance to maintain the speed at the desired value. To compute the applied torque, we use the result of solving the vertical oscillation from (8), and also the sum of the touchdown angles computed in (9). So the applied torque is provided by the function f_2:

$$\tau=f_2(\underbrace{m,k,L,d,I,b,g}_{\text{robot parameters}},\ \underbrace{\dot{x}_{des},h}_{\text{gait parameters}},\ \underbrace{\gamma_{sum,td}}_{\text{control parameter}}) \quad (11)$$

C. Pitching motion

In [10], the pitching motion is predicted by the equation:

$$I_b\ddot{\theta}+2d^2b\dot{\theta}+2d^2k\theta=$$
$$2kLd\sin\left(\frac{\gamma_{sum,td}}{2}-\frac{\dot{x}t}{L}\right)\sin\left(\frac{\gamma_{dif,td}}{2}\right)-\tau_b-\tau_f \quad (12)$$

Here, we observe again that the governing dynamics have the form of a driven oscillator. The control must keep the pitching motion of the robot to a minimum. We use the pitch control approach developed in [10], with the difference that the inertia and motion of the two legs not involved in the stance phase must be taken into account. The difference of the leg touchdown angles is computed so as to suppress deviations of pitching from the zero value:

$$\gamma_{dif,td}=f_3(\underbrace{m,k,L,d,I,b,g}_{\text{robot parameters}},\ \underbrace{\dot{x}_{des},h}_{\text{gait parameters}},\ \underbrace{\gamma_{sum,td},\tau}_{\text{control parameters}}) \quad (13)$$

D. Control implementation

In this section we explain in detail how the control is implemented in practice, and the sequence of events. Sensors on the robot provide leg angle position and velocity, leg length and velocity, and body pitch and pitch velocity. The quantities associated with the legs may be measured with rotary and linear encoders respectively, while successful experiments measuring pitch or even using pitch feedback are already available in the literature [11,3,2].

With reference to Fig. 3, we can follow through the control sequence, to outline how it would work and to better understand the parametric analysis that follows.

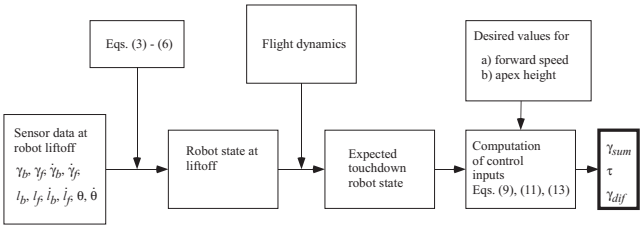

Fig. 3. Sequence of control computations that give the control inputs, i.e the leg touchdown angles and the constant hip torque applied during stance.

Let us now assume that the robot is at the point of liftoff from the ground. Using sensor data and robot geometry the full robot state is known, i.e by solving (3) to (6) for the

robot states using on-board computing, see Fig. 3b. Once the state at liftoff is known, the flight dynamics is relatively simple to integrate, and so the expected touchdown state of the robot can be found, Fig. 3c. Next, the three functions in (9), (11), (13) are used to compute $\gamma_{sum,td}$, τ, and $\gamma_{dif,td}$, such that at the next apex point, the robot will have the desired forward speed, height, and zero pitching.

E. Control Application Example

As a simple demonstration of the viability of the control method, a simulation of a quadruped robot in the 3D simulation software ADAMS is shown here, with the motion of the robot body constrained to the plane of forward motion. The control drives the robot to a desired forward speed and apex height, while retaining a limited pitching motion. The robot response is shown in Fig. 4.

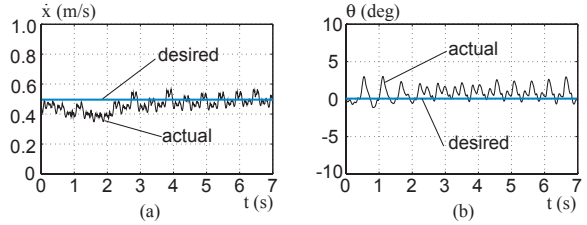

Fig. 4. Robot response to the controller in Fig. 3, in a 3D simulation in ADAMS. Speed control at 0.5m/s. (a) Forward speed, (b) body orientation.

IV. Parametric Study

The parametric study focuses on the actuator effort and the sum of the leg touchdown angles, referred to in the following as the Parametric Study (PS) variables. In particular, we examine how the PS variables change as a function of a range of robot physical parameters, such as body mass or leg length, and also for a range of gait characteristics, meaning the forward speed and apex height.

To implement the parametric study, the PS variables must be calculated for many different robot physical parameters and gait characteristics. To obtain a single set of values for the PS variables, the control algorithm in Fig. 3 is applied to the robot with the given physical parameters. The given forward speed and apex height are fed to the controller, and the system is simulated using Matlab. Once the robot enters a steady-state motion, the PS variables are known from the simulation data. Typically, the robot enters a steady-state motion after about 10 cycles of trotting.

One of the PS variables is the actuator effort. The actuator effort study is restricted to the actuator effort during the stance phase. The reason for this is that leg positioning during flight was done using a bang-bang type control which always applied torques of the same magnitude, over all parametric regions, changing only their duration. Therefore, there was no benefit to including them in the parametric study. When sizing the robot actuators, the magnitude of flight phase actuator effort can be regarded as a constant condition that must be fulfilled.

The advantages of the control algorithm in Fig. 3 for implementing the parametric study are now apparent. Controlling both the forward speed and the apex height was necessary to obtain values for the PS variables over the parametric regions. The control's parametric form makes it simpler to apply for a variety of robot physical parameters and gait characteristics. Also, as the actuators apply constant torques during stance, the actuator effort can be directly compared over the parametric region.

It is anticipated that the results of the parametric study are largely indifferent to the particular type of control applied to the robot. Part of the reason for this is that the robot studied only has one actuator per leg. In this case, little of the robot's natural dynamics can be forced by any type of control. Due to the high underactuation, the control can only attempt to stimulate internal dynamic mechanisms. Additionally, due to parametric form of the control, the control algorithm coefficients are recomputed for every set of robot parameters. In this sense, one may say that the control is optimized for each robot. As a result of the above, the conclusions of the study should hold qualitatively for many types of control.

Finally, the problem to be studied involves a large number of parameters, leading to many potential case studies, but our aim here is to illustrate the most interesting findings. The study is split into two main cases. In the first case, specific gait characteristics are given, and preferred regions of robot physical parameters are sought for this gait. The second case considers a robot with given physical parameters, and identifies regions of gait characteristics that are advantageous for this robot.

A. Evaluating a robot design for a given gait

First, let us examine the variation of the sum of the leg touchdown angles, $\gamma_{sum,td}$, for a robot body mass range. The remaining physical parameters of the robot are kept constant and the same applies to the desired apex height. With reference to the symbols in Table 1, the robot has k_b =6000 N/m, d =0.25 m, L =0.3 m and b =10 N·s/m.

In Fig. 5, it can be seen that $\gamma_{sum,td}$ increases as the body mass increases, for three forward speeds. Since the robot is more prone to slip as the legs hit the ground with larger angles, it would be preferable for the robot to be lighter-weight when running on slippery terrain. It is perhaps interesting that, for different reasons, the opposite technique is often used to improve traction for wheeled vehicles.

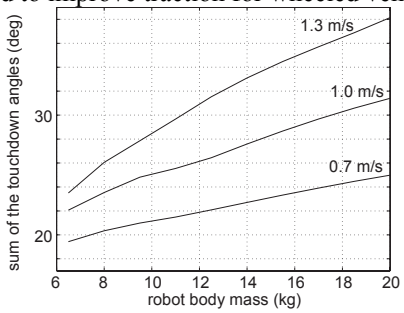

Fig. 5 Sum of the leg touchdown angles used for a range of the body mass, and for three different forward speeds. The touchdown angles increase with robot mass and speed.

The reason for this increase in $\gamma_{sum,td}$ is due to the larger mass causing a greater deflection of the spring during stance, which generally leads to larger losses. As the robot is unactuated in the prismatic joint, to pump energy into this DOF, the legs must hit the ground with greater angles. This pumping mechanism is described in [12].

Result 1: For lower-friction terrain, it is preferable for a robot to be lighter-weight.

It is also interesting to examine what happens in the case where the ratio of the spring stiffness over the mass of the robot body remains constant. This ratio is often referred to as the relative stiffness of the system, and gives a measure of how hard the leg spring is, indifferent of the absolute value of the spring stiffness. For three different *constant* values of relative stiffness, the sum of the leg touchdown angles $\gamma_{sum,td}$ is plotted versus the robot body mass, in Fig. 6. Note that the x axis represents a change in both the body mass *and* the spring stiffness, so that the relative stiffness remains constant. As can be seen, the value for $\gamma_{sum,td}$ decreases with robot body mass, for a constant relative stiffness. This demonstrates that important parameters of the robot motion vary, even while retaining a constant relative stiffness. It also appears that having a stiffer system, i.e a larger relative stiffness, leads to smaller values for $\gamma_{sum,td}$, for the same robot body mass.

Result 2: The sum of the leg touchdown angles decreases for systems with higher relative stiffness.

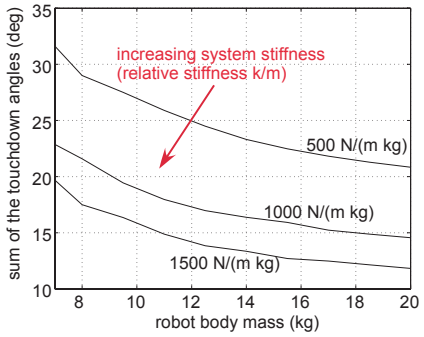

Fig. 6 The sum of the touchdown angles over the robot body mass, for three *constant* values of the relative stiffness (500 N/(m·kg), 1000 N/(m·kg), 1500 N/(m·kg)). The sum of the touchdown angles decreases for stiffer systems, for the same body mass.

Another key physical parameter of the robot is the length of the legs. In Fig. 7, the required hip joint torque during the stance phase was computed in steady-state running, for various lengths of the robot leg. It is evident that there is a strong correlation between the required torque and the length of the leg. In Fig. 7, the data is gathered for three forward speeds, ranging from 0.7 m/s to 0.9 m/s. It can be seen that dependence on speed is not particularly significant in this range, when compared to the large variations over the leg length. The mechanism behind this result is simple; as the leg lever increases, more torque is needed to produce the same forward force. Consider a typical actuator setup, such as a 24V 60W DC motor of Maxon Motors, combined with a planetary gear with a ratio of 50. The torque that this combo can continuously provide is 4.3Nm. In Fig. 7, the shaded area shows unachievable region using the above actuator. Observing Fig. 7, one can notice that for speeds down to 0.7 m/s, leg lengths of up to 0.35 m can be used.

Result 3: The greatest leg length that may be used is limited by the maximum torque of the actuator and the minimum desired speed for the robot.

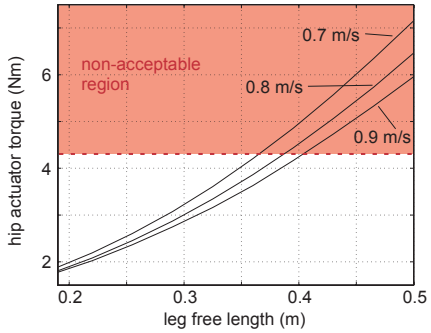

Fig. 7 The hip actuator torque, for various values of the free length of the robot leg, and for three different forward speeds. The actuator hip torque increases with the leg free length. The shaded area shows the region that is not achievable with a particular actuator setup, described in the text.

B. Evaluating a gait for a given robot

Now, let us examine the case of a robot with predefined physical parameters, in which case the parametric region of interest is limited to the gait characteristics. The aim is to identify whether some regions of gaits are advantageous, either regarding the required actuator effort, or the possibility of slipping, which is directly connected to the value of the touchdown angles of the legs. The robot has the physical parameters laid out in part A of this section, and a body mass of 15 kg.

First, consider the case for which a particular apex height is desired. The required torque during the stance phase is shown in Fig. 8, for a range of forward speeds and for three different values of the apex height. For each apex height, in the range of speeds studied, there is a systematic decrease in the torque as the forward speed increases.

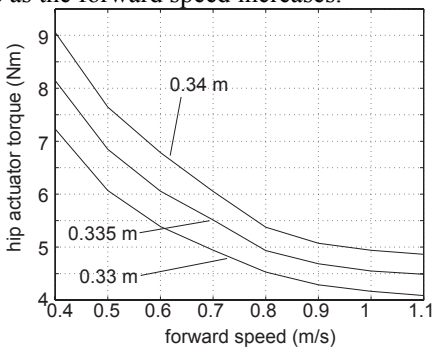

Fig. 8 The hip actuator torque, for various forward speeds of a robot. The data is shown for three different apex heights. The hip actuator torque appears largest for smaller speeds.

It is expected that this decrease of actuator torque as a function of forward speed will not continue indefinitely. However, Fig. 8 is interesting as it demonstrates that slower speeds do not necessarily require lower torques, as may be expected. Note that the power consumed by the actuator

does not necessarily decrease with speed, as the revolving speed of the leg will increase with forward speed and the power is proportional to this speed. Despite the fact that power consumption may increase, the actuator torque is important for sizing the actuators. If the robot uses batteries, their function is also affected by these results, as the torque required is proportional to the electrical current drawn. Therefore it may be beneficial when running long distances to run at a speed at which the batteries discharge optimally.

To interpret the result in Fig. 8, it is useful to recall the concept of the "neutral point" from Raibert's work [7]. The neutral point represents the angle with which the studied robot leg would touchdown for steady forward running at some speed. As our robot has only one actuator per leg and not two, as in [7], the touchdown angles used by our control are expected to differ. *At* the neutral point, as defined in [7], the sum of the leg touchdown angles for our robot would be:

$$\gamma_{sum,td} = \dot{x} \cdot T_{st} / L \qquad (14)$$

The sum of the touchdown angles in (14), $\gamma_{sum,td}$, corresponding to the neutral point, is plotted in Fig. 9 with crosses, for the same case as in Fig. 8. Also, the actual sum of the touchdown angles used is plotted in Fig. 9 with black curves. As predicted the two differ, but increasingly less as the speed increases. This is seen by plotting the difference of the two with red circles. The fact that the actual $\gamma_{sum,td}$ used is much greater than that of the neutral point at smaller speeds means that at those speeds there is more resistance to the forward motion, as the foot lands further forward at touchdown [7]. This results in larger required torques at smaller speeds, to overcome the greater resistance.

Result 4: Smaller speeds can require much higher actuator effort than moderate speeds, as the leg touchdown angles deviate more from the "neutral point" at small speeds.

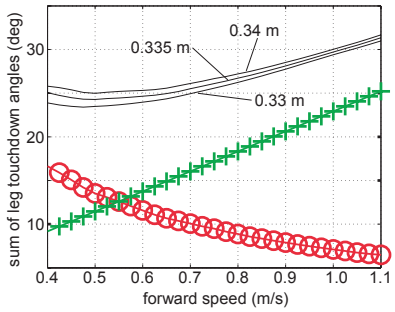

Fig. 9 Sum of the leg touchdown angles, for a range of forward speeds and for three different apex heights (black curves). Also, the sum of the touchdown angles corresponding to Raibert's "neutral point" is shown for the apex height of 0.34m (green crosses). Finally, the difference of the two is shown, again for the apex height of 0.34 m (red circles).

Finally, it is worth mentioning the minimum that appears in the sum of the leg touchdown angles in Fig. 9. This minimum, which occurs at about 0.5 m/s for all three apex heights studied, suggests that this may be the best speed to use when running on surfaces with less friction, as the legs are more prone to slip for larger touchdown angles.

Result 5: There exists an optimal speed to run at when on lower-friction terrain, which is neither very slow nor fast.

CONCLUSIONS

For the case of a trotting quadruped robot, a novel controller was developed, specially suited to a parametric analysis of the robot. The control was shown to be capable of setting both robot forward speed and attained apex height, using only one actuator per leg. The parametric study itself followed and led to a number of findings. On one hand, a given robot was studied for a variety of gait characteristics. On the other hand, the influence of robot physical parameters was considered for the cases were a specific gait is desired. Interesting findings included that (a) the mass of a running robot should be reduced when running on a lower-friction terrain, (b) the sum of the leg touchdown angles increase as system stiffness increases, (c) the largest possible leg length for a robot is limited by the actuator torque limit and the lowest desirable speed of the robot, (d) some higher running speeds may require less actuator torque than for smaller speeds, (e) there is an optimal speed for running when on low friction terrain. These findings could assist with the design or modification of quadruped robots, as well as with the selection of the most suitable gaits for a robot.

REFERENCES

[1] D. Papadopoulos and M. Buehler, "Stable running in a quadruped robot with compliant legs," *Proc. 2000 IEEE Int. Conf. Robotics and Automation*, pp. 444-449, 2000.

[2] Z. G. Zhang, T. Masuda, H. Kimura and K. Takase, "Towards Realization of Adaptive Running of a Quadruped Robot Using Delayed Feedback Control", *Proc. Of the 2007 IEEE Conference on Robotics and Automation*, pp. 4325-4330, 2007.

[3] H. Kimura, Y. Fukuoka and A. H. Cohen, "Adaptive Dynamic Walking of a Quadruped Robot on Natural Ground Based on Biological Concepts," *The International Journal of Robotics Research*, vol. 26, no. 5, pp. 475-490, 2007.

[4] R. Playter, M. Buehler and M. Raibert, "BigDog," *Proc. of SPIE Defense & Security Symposium*, Volume 6230, Unmanned Systems Technology VIII, G. R. Gerhart, C. M. Shoemaker, D. W. Gage, Eds., 2006.

[5] J. G. Nichol, S. P. N. Singh, K. J. Waldron, L. R. Palmer III, D. E. Orin, "System Design of a Quadrupedal Galloping Machine," *The International Journal of Robotics Research*, vol. 23, no. 10-11, pp. 1013-1027, 2004.

[6] E. Papadopoulos and N. Cherouvim, "On Increasing Energy Autonomy for a One-Legged Hopping Robot," *Proc. Of the 2004 IEEE Conference on Robotics and Automation*, pp. 4645-4650, 2004.

[7] M. H. Raibert, "Legged robots that balance," *MIT Press*, Cambridge, MA, 1986.

[8] I. Poulakakis, E. Papadopoulos and M. Buehler, "On the Stability of the Passive Dynamics of Quadrupedal Running with a Bounding Gait," *The International Journal of Robotics Research*, vol. 25, no. 7, pp. 669-687, 2006.

[9] M. D. Berkemeier, "Modeling the Dynamics of Quadrupedal Running," *The International Journal of Robotics Research*, vol. 17, no. 9, pp. 971-985, 1998.

[10] N. Cherouvim and E. Papadopoulos, "Pitch Control for Running Quadrupeds Using Leg Positioning in Flight," Proc. 15th IEEE Mediterranean Conference on Control and Automation, 2007.

[11] N. Neville, M. Buehler and Inna Sharf, "A Bipedal Running Robot with One Actuator per Leg," *Proc. 2006 IEEE Int. Conf. Robotics and Automation*, pp. 848-853, 2006.

[12] N. Cherouvim and E. Papadopoulos, "Single Actuator Control of a 3DOF Hopping Robot," *Chapter in Robotics: Science and Systems I*, Thrun et al. (Eds.), MIT Press, Cambridge, MA, 2005.